PAPER

The effects of geochemical processes on groundwater chemistry and the health risks associated with fluoride intake in a semi-arid region of South India

D. Karunanidhi, [iD] *[a] P. Aravinthasamy,[a] M. Deepali,[b] T. Subramani[c] and Priyadarsi D. Roy[d]

This study attempts to establish the effects of subsurface geochemical processes based on the hydrogeochemical attributes of 61 well samples collected in a semi-arid region of South India. The study also provides the health risks associated with the consumption of fluoride-enriched groundwater by the rural people since groundwater is the major source of water supply in the Shanmuganadhi River basin. In this work, water–rock interaction diagrams, an entropy-weighted water quality index (EWQI), and health risk models as per the United States Environmental Protection Agency (USEPA) were prepared to understand the geochemical mechanism behind the groundwater chemistry and its role in impacting health. About 72% of these samples are of mixed $Ca^{2+}-Mg^{2+}-Cl^-$ water type, representing a transition from freshwater to brackish water, and 36% of them have fluoride above the permissible limit (>1.5 mg l^{-1}). An evaluation of the hydrogeochemical attributes suggests that silicate weathering, carbonate dissolution and reverse ion exchange mostly control the hydrochemistry of the groundwater. The EWQI characterizes about 30% of these samples as unsuitable for drinking and another 49% as of moderate quality. Human health risks were evaluated by dividing the population into seven different age groups and estimating the hazard quotient (HQ) and total hazard index (THI) from intake and dermal contact with fluoride-rich groundwater. The groundwater of this region poses a higher risk for the younger population compared to the adults. About 79% of these groundwater samples pose a health risk to 5–12 month-old infants and only 36% of the samples could be potentially hazardous for adults >23 years old. Our results suggest that the ADD_{dermal} pathway indicates less risk compared to the ADD_{intake} estimations.

1. Introduction

Both surface and groundwater play important roles in shaping the quality of lives and sustainability of societies.[1] Surface water is scarce and its quality is poor in arid and semi-arid regions, and thus groundwater is used in these water-scarce regions for drinking and irrigation purposes.[2] The exploitation of groundwater is rapidly growing for domestic, industrial and irrigation use owing to population expansion across the globe. It has caused depletion in groundwater reserves, water quality impairment issues and higher withdrawal costs.[3–5] The quality of groundwater is influenced by natural and anthropogenic

activities and restoring the original quality of already contaminated groundwater is very difficult. Groundwater's poor quality with respect to arsenic, fluoride, chromium and many other pollutants increases human health risks.[6–9] Fluoride in drinking water has created serious health issues in human beings.[10–14] It is sourced from the interaction of the groundwater with fluoride-bearing minerals[15,16] and its concentration depends upon the physicochemical parameters of the groundwater and other factors and processes, such as evapotranspiration, anion exchange, the solubility of fluoride-bearing minerals and precipitation.[17–20] Higher concentrations (>1.5 mg l^{-1}) of this ion of fluorine (halogen group) give rise to dental fluorosis and skeletal fluorosis.[21,22] It has been reported that about 400 million people are exposed to artificially fluoridated water.

The groundwater from mid-altitude subtropical regions has higher fluoride owing to warmer conditions, enhanced evaporation and less rainfall.[15,23,24] Several parts of India, Iraq, Libya, Turkey, China, Sri Lanka, USA, Pakistan, Iran, East Africa's Rift Valley, Scandinavia and Canada have fluoride-enriched water.[25–30] About 66 million people in India living in 250

[a]*Department of Civil Engineering, Sri Shakthi Institute of Engineering and Technology (Autonomous), Coimbatore – 641062, India. E-mail: karunasamygis@gmail.com; Tel: +91 9786557646*

[b]*Department of Applied Chemistry, Priyadarshini Institute of Engineering and Technology, Nagpur – 440019, India*

[c]*Department of Geology, CEG Campus, Anna University, Chennai – 600025, India*

[d]*Instituto de Geología, Universidad Nacional Autónoma de México (UNAM), Ciudad Universitaria, CP 04510, Mexico City, Mexico*

districts are at risk of endemic fluorosis and 25 million of them (mostly <18 years) have dental fluorosis.[31] The improved water quality index (IWQI) or the EWQI, which includes the entropy-weighted value, have been used by various researchers to quantify the fluoride concentration in groundwater water[32–35] and to rank and classify water quality[36] using the entropy TOPSIS method. Similarly, researchers have defined the impact of fluoride-rich groundwater consumption by considering two
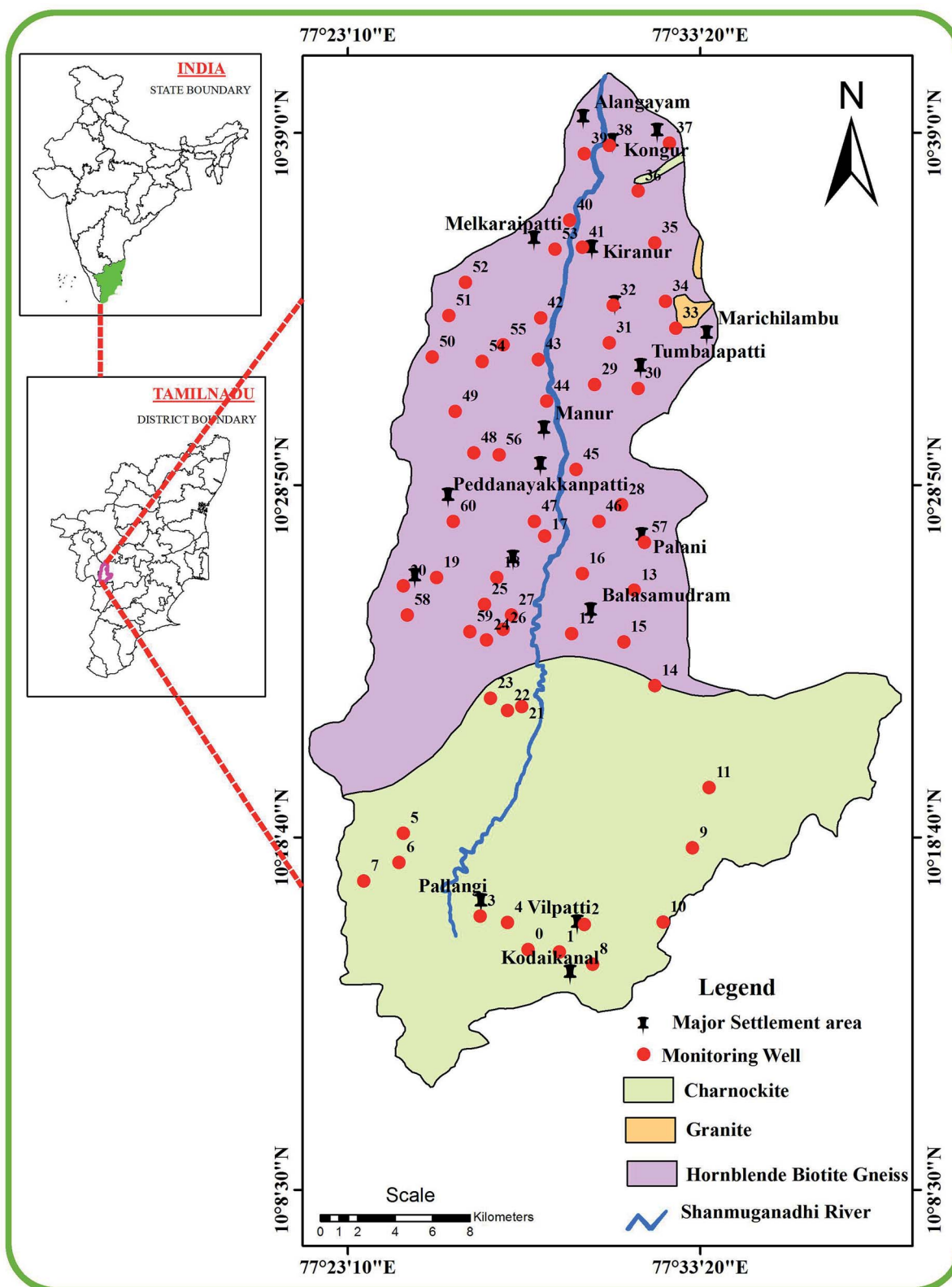

Fig. 1 Groundwater samples collected from different geological formations in the Shanmuganadhi River basin of South India.

Table 1 Parameters considered for risk evaluation based on fluoride intake and dermal contact among different age groups in a semi-arid basin of South India

Parameter	Unit	5–12 months	5–13 years	14–16 years	17–20 years	21–23 years	>23 years	>65 years
Water intake rate (IR)	ml per day	1	1.32	1.82	1.78	2.34	2.94	2.73
Average time (AT)	Days	2190	2190	2190	2190	10 950	10 950	10 950
Exposure frequency (EF) oral	Day per year	365	365	365	365	365	365	365
Exposure duration (ED)	Year	6	6	6	6	30	30	30
Body weight (BW)	kg	9.1	29.3	54.2	67.6	67.6	78.8	80
Skin surface area (SA)	cm^2	4500	10 500	15 700	18 000	19 550	19 800	19 400
Exposure time (ET) dermal	h per event	0.54	0.54	0.54	0.54	0.71	0.71	0.71
Exposure frequency (EF) dermal	Day per year	350	350	350	350	350	350	350
Conversion factor (CF)	l cm^{-2}	0.001	0.001	0.001	0.001	0.001	0.001	0.001
Skin adherence factor (kp)	cm h^{-1}	0.001	0.001	0.001	0.001	0.001	0.001	0.001
Oral reference dose (RfD$_0$)	mg per kg per day	0.06	0.06	0.06	0.06	0.06	0.06	0.06
Concentration of element (C)	mg l^{-1}	Present study						

common pathways (intake and dermal) as per the USEPA health risk model.[18,22,37–39]

The present study was carried out to (i) identify the major geochemical processes and anthropogenic sources of F$^-$ from hydrogeochemical parameters, (ii) delineate fluoride-vulnerable zones using spatial distribution maps, (iii) rank the groundwater quality for drinking utilities using the entropy water quality index (EWQI) and (iv) assess the human health risk of fluoride-enriched groundwater from oral and dermal intake pathways in seven age groups (i.e., 5–12 months, 5–13 years, 14–16 years, 17–20 years, 21–23 years, ≥23 years and >65 years) in a semi-arid part of South India, with the principal objective of effective water utilization and groundwater protection.

2. Study area

2.1 Location and climate

Several states in the southern part of India (e.g., Telangana, Tamil Nadu, Kerala and Andhra Pradesh) are prone to fluorosis.[19,40] The study region is situated in the west part of Tamil Nadu, encompassing an area of 807.52 km^2 between the latitudes of 10°11′–10°40′ N and longitudes of 77°21′–77°40′ E (Fig. 1). It has a tropical climate with dry and warm conditions (29–37 °C) during April–June and relatively cool conditions (20–26 °C) in November–January. It has humidity of 65–85% during the morning and 40–70% in the afternoon.[41] The area is considered drought-prone owing to its location in the rain shadow of the Western Ghats Mountains. This arid or semi-arid region receives an average annual rainfall of 760–910 mm and most of its water budget is controlled by the surface and groundwater resources fed by the ephemeral Shanmuganadhi River, which originates in the Kodai hills and flows for nearly 56 km from the south to north. Red soil, black cotton soil, and red sandy soil are used for cultivation of finger millet, tomatoes, maize, spinach, beans, cassava and other vegetable/leguminous crops during the cooler months and the cultivation of sugarcane, rice, guinea-corn and maize in the wetter months.

Table 2 Physicochemical parameters of groundwater samples in the study area and the desirable and permissible limits as per the WHO

Parameter	Unit	Maximum	Mean	WHO 2017	
				Most desirable	Not permissible
EC	μS cm^{-1}	3040	1150.1	<1500	>1500
TDS	mg l^{-1}	2128	805.1	<500	>1500
pH	—	8.13	7.5	6.5 to 8.5	<6.5 and >8.5
TH	mg l^{-1}	792	293.1	<450	>450
Calcium	mg l^{-1}	174.4	70.8	<75	>200
Magnesium	mg l^{-1}	85.44	27.9	<50	>150
Sodium	mg l^{-1}	300	116.6	<200	>200
Potassium	mg l^{-1}	100	25.0	<10	>10
Bicarbonate	mg l^{-1}	488	214.9	<300	>600
Chloride	mg l^{-1}	656	129.7	<200	>600
Sulphate	mg l^{-1}	395	133.5	<400	>400
Nitrate	mg l^{-1}	75	30.9	<45	>45
Phosphate	mg l^{-1}	2.9	0.3	<0.3	>0.3
Fluoride	mg l^{-1}	3.7	1.3	<1.5	>1.5

2.2 Geohydrology

The geology of the Shanmuganadhi River is mainly composed of hornblende biotite gneiss and charnockite with minor amounts of exposed.[42] Charnockite is present in the upstream area and the hornblende biotite gneisses are confined to the southern parts along the downstream. The aquifers are characterized by an open system of weathered porous zones and an un-weathered portion with joints and fissures. The groundwater is confined to the weathered and fractured zones of the char-nockite as well as the hornblende biotite gneiss. The fracture zones are confined to 68–120 m below the ground, irrespective of the lithologies. However, the average depth of the bore wells ranges from 25 to 37 m and the groundwater is mostly tapped from the phreatic aquifer through open wells for irrigation purposes. Most of these wells are confined to the semi-confined fracture zones.

3. Materials and methods

3.1 Groundwater sampling

The locations of the groundwater samples ($n = 61$) were marked with the help of six different 1 : 50 000 scale Survey of India (SOI) toposheets (58-F/12, 58-F/11, 58-F/10, 58-F/08, 58-F/07 and 58-F/06) and digitized using ArcGIS software (v.10.2.1). All of the
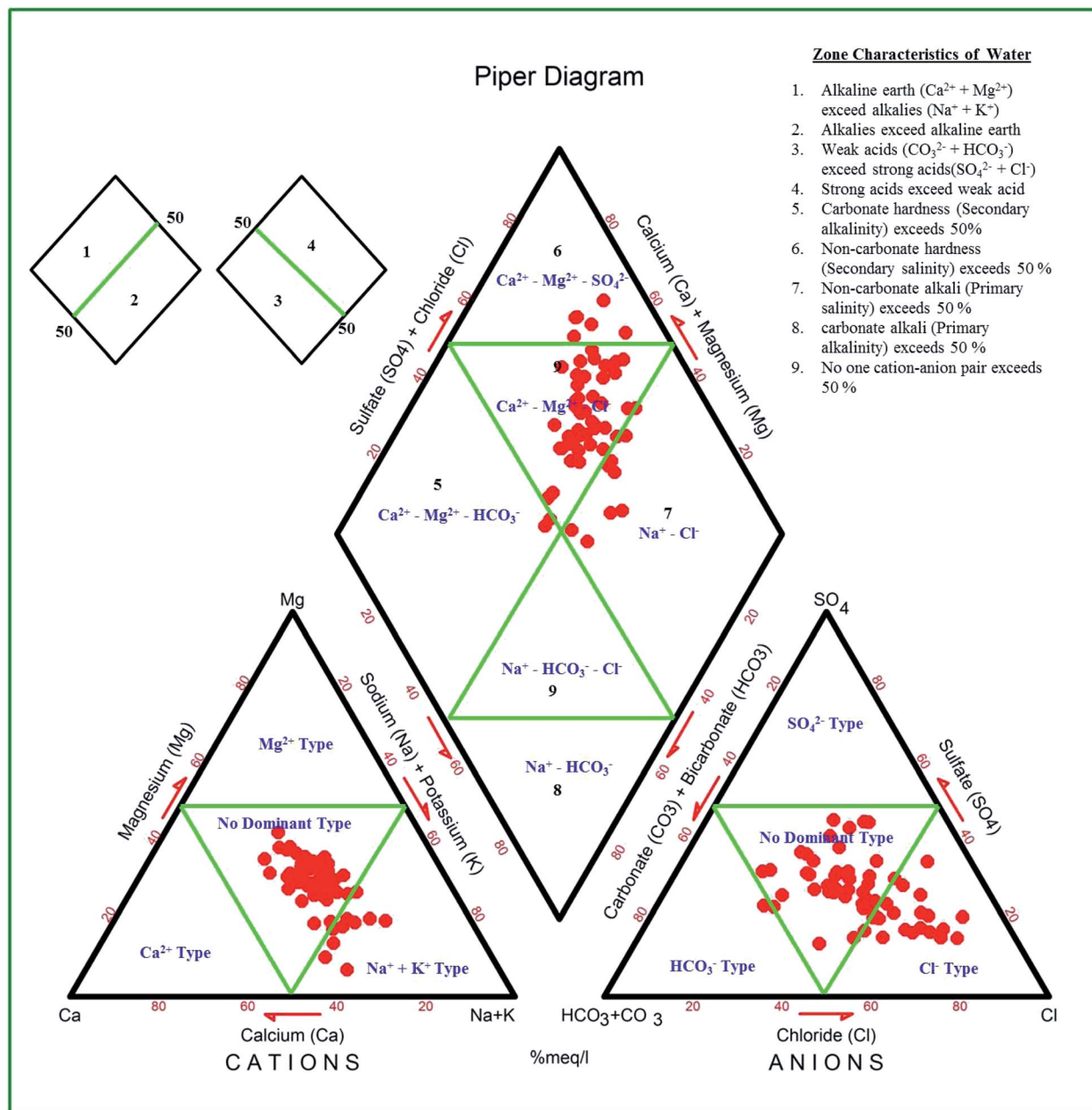
Fig. 2 Groundwater types in the study area from the Piper diagram.
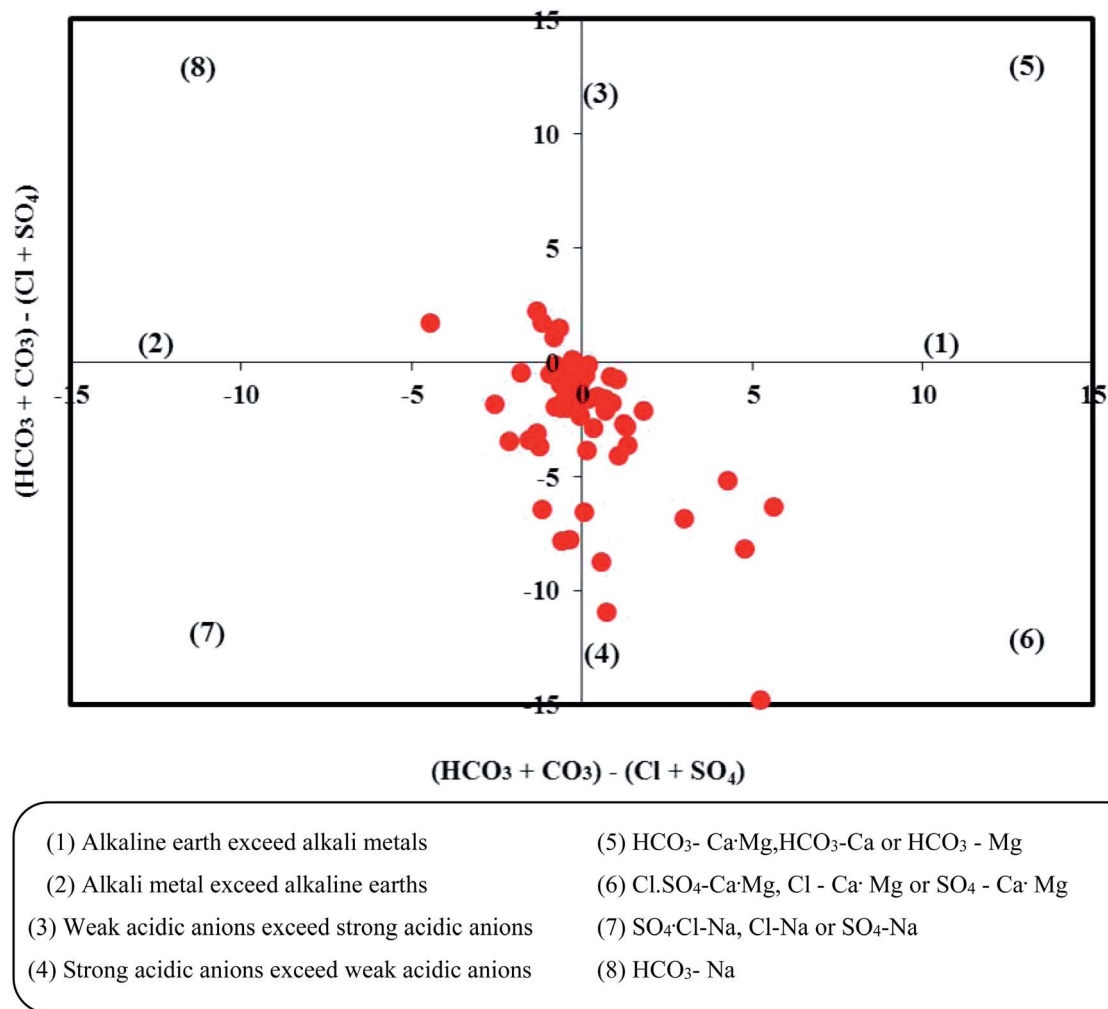
Fig. 3   Groundwater types in the study area based on the Chadha diagram.

samples were collected (May 2019) from the dug and bore wells in pre-cleaned Teflon bottles without any air bubbles and properly closed with stoppers and then brought to the laboratory for further chemical analysis.

3.2   Analytical procedures

The samples were analyzed for different hydrogeochemical parameters.[43] The pH, EC, and TDS values were analyzed using an *in situ* water quality analyzer (ESICO MODEL 1160E). The chloride concentrations were estimated by titration using silver nitrate and HCO_3^- was measured using titrimetry.[43] Similarly, the concentrations of Ca^{2+} and Mg^{2+} were measured by EDTA solution and the concentrations of K^+ and Na^+ were analyzed using a flame photometer. The contents of NO_3^-, SO_4^{2-} and PO_4^- were analyzed using a UV-visible spectrophotometer. An ion-selective electrode (LMION-40) was used to determine F^- in the groundwater samples. The accuracy of the results was determined by checking the ion balance using eqn (1) (all the ions are in meq l^{-1}) and the calculated EIB are within the permissible limit of $\pm 10\%$.

$$EIB = \frac{\sum Cations \; - \; \sum Anions}{\sum Cations \; + \sum Anions} \times 100 \quad (1)$$

3.3   Entropy water quality index (EWQI)

The entropy water quality index (EWQI) was calculated using eqn (2):[33]

$$EWQI = \sum_{j=0}^{n} w_j q_j \quad (2)$$

where n express the number of parameters selected to calculate the EWQI, w_j denotes the entropy weight of the jth parameter, and q_j denotes the quality rating scale of the jth parameter.

The entropy weight (w_j) of each parameter was calculated using eqn (3):[44]

$$w_j = \frac{1 - e_j}{\sum_{j=1}^{n} (1 - e_j)} \quad (3)$$

The information entropy (e_j) of the jth parameter can be determined using eqn (4):

$$e_j - = \frac{1}{\ln m} \sum_{i=1}^{m} P_{ij} \ln P_{ij} \qquad (4)$$

where m denotes the total number of samples and P_{ij} is the ratio of the index value for the j index in sample i and is computed using eqn (5):[45]

$$P_{ij} = \frac{y_{ij} + 0.0001}{\sum_{i=1}^{n}(y_{ij} + 0.0001)} \qquad (5)$$
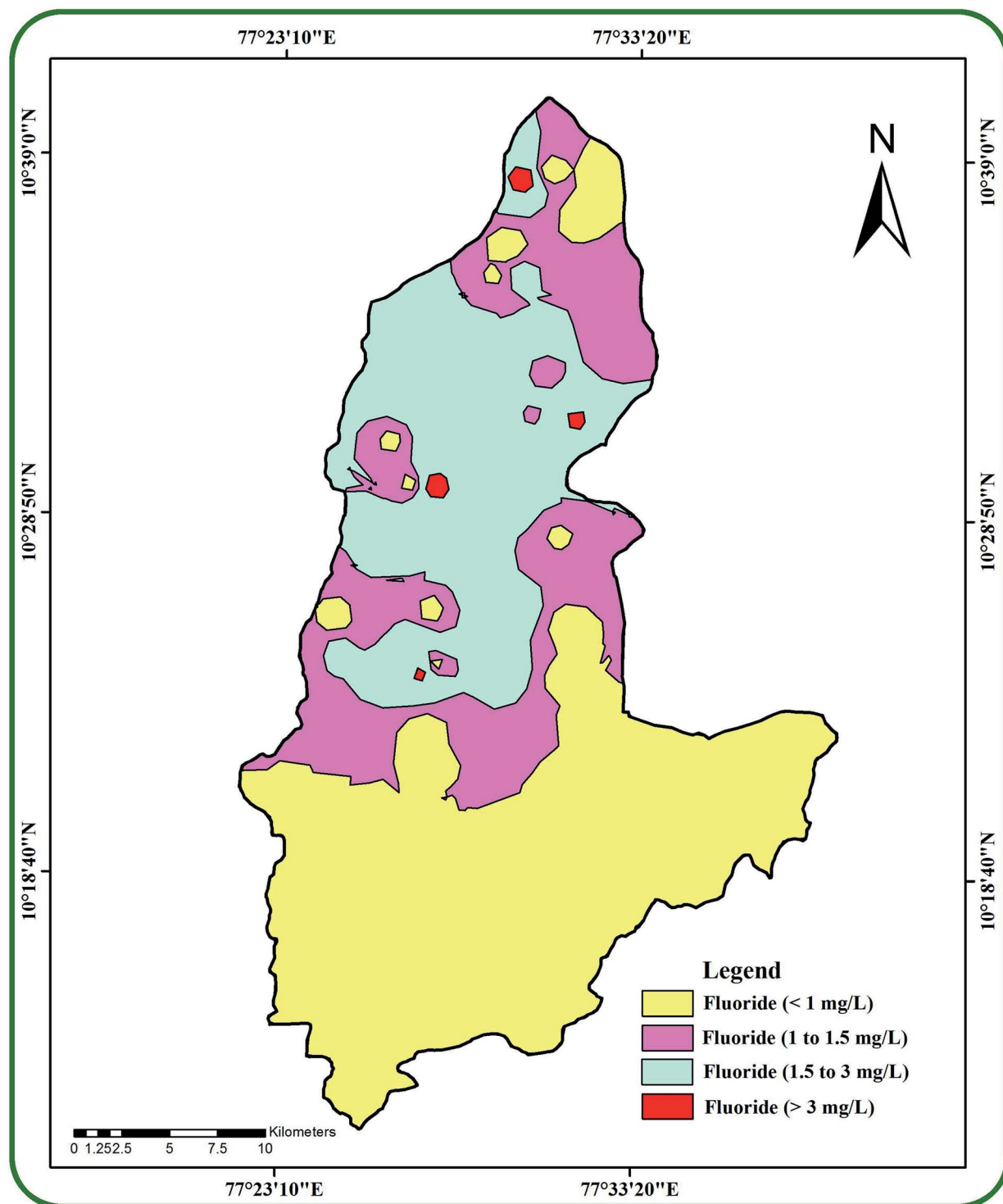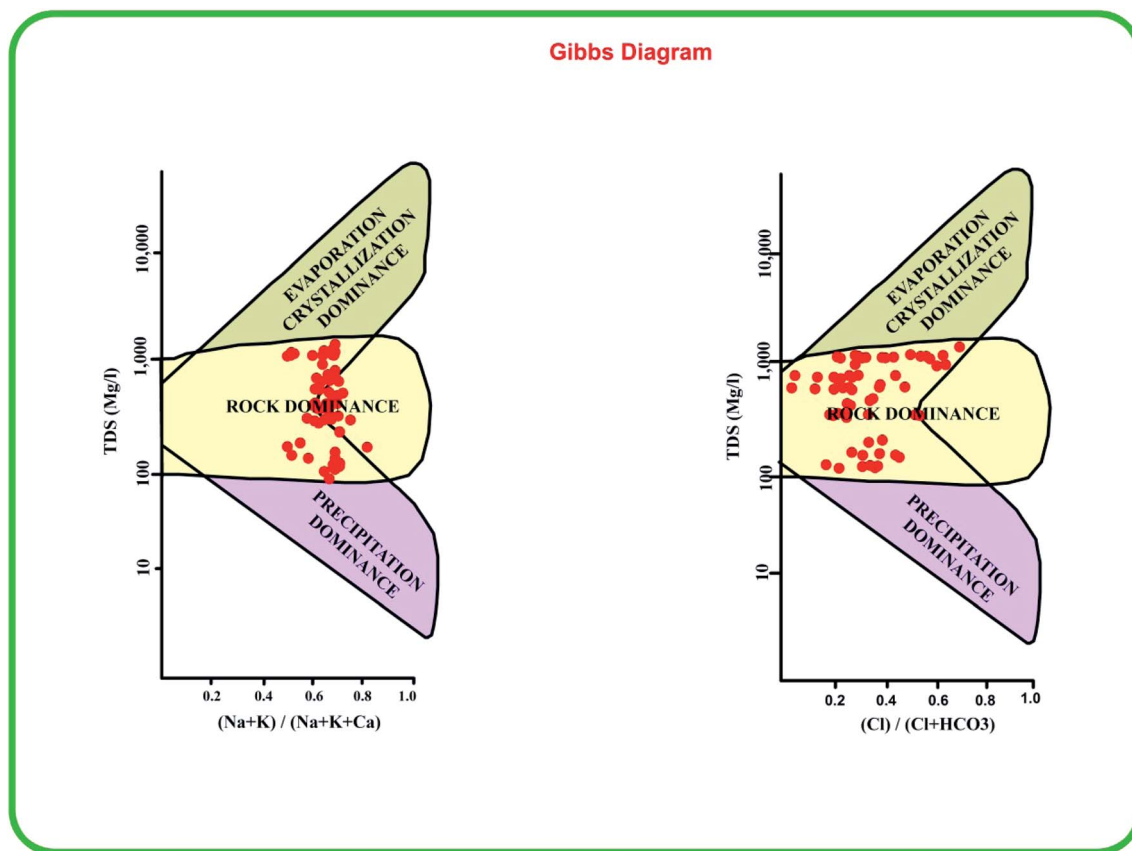

Fig. 4 The spatial occurrence of fluoride in the groundwater of the study area.

Fig. 5   Gibbs plots indicating the dominant hydrogeochemical factors affecting the groundwater chemistry in the study area.

where y_{ij} is the standardized value of the jth parameter for the ith sample, and they are determined by using eqn (6) and (7):

$$y_{ij} = \frac{C_{ij} - C_j^{min}}{C_j^{max} - C_j^{min}} \text{ (for efficiency type paramaters)} \quad (6)$$

$$y_{ij} = \frac{C_j^{max} - C_{ij}}{C_j^{max} - C_j^{min}} \text{ (for cost type parameters)} \quad (7)$$

where C_{ij} denotes the detected value of the jth parameter for the ith sample, and C_j^{max} and C_j^{min} denote the maximum and minimum values of the jth parameter, respectively.
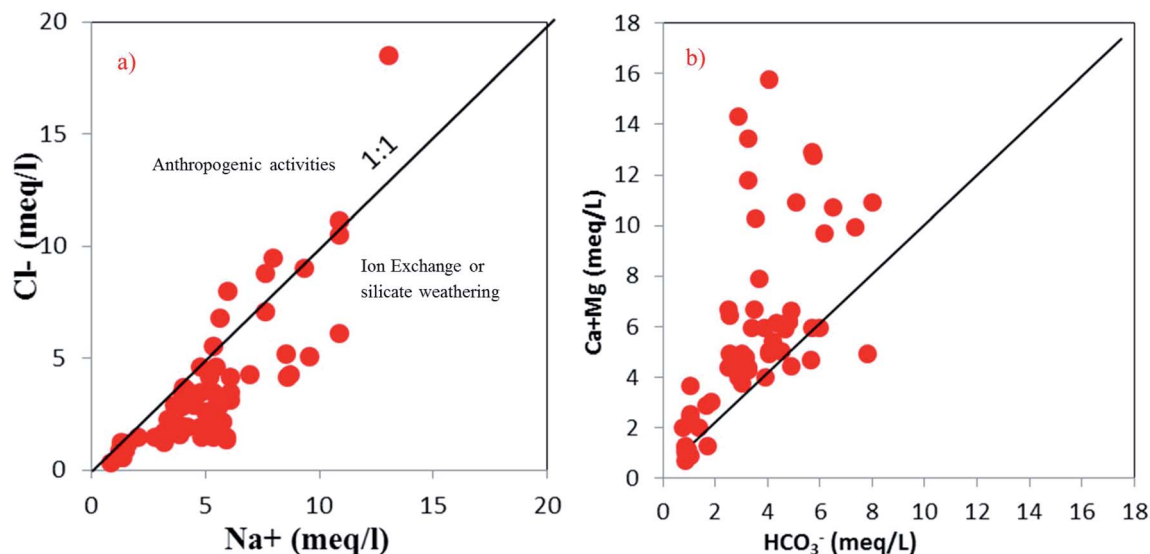
Fig. 6   Scatter plots (a and b) indicating the effects of silicate weathering on groundwater chemistry.
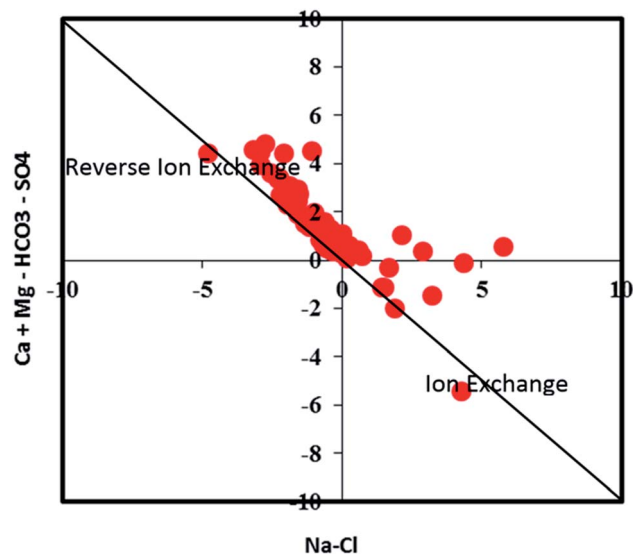
Fig. 7   A scatter plot indicating the groundwater samples representing positive and reverse ion exchange processes.

Fig. 9   A scatter plot illustrating carbonate and sulfate dissolution.

The last step in calculating EWQI is to assign a quality rating scale (q_j) for each parameter based on the concentration of each chemical parameter (C_j) in mg l^{-1}; S_j is the desirable limit for a particular parameter in mg l^{-1} according to the WHO standards.[32] q_j is calculated using eqn (8):

$$q_i = \frac{C_j}{S_j} \times 100 \qquad (8)$$

3.4   Health risk assessment model

The health risks assessment are estimated by considering consumption of water through ingestion and dermal paths for seven different age groups (i.e., 5–12 months, 5–13 years, 14–16 years, 17–20 years, 21–23 years, ≥23 years, and >65 years; Table 1).[46] We attempted to determine the fluoride ingestion via dermal contact by considering the average daily dose (ADD) and HQ (hazard quotient) using eqn (9)–(12):[47–49]

$$ADD_{intake} = \frac{C \times IR \times EF \times ED}{BW \times AT} \qquad (9)$$

$$ADD_{Dermal} = \frac{C \times ESA \times K \times EF \times ED \times CF}{BW \times AT} \qquad (10)$$
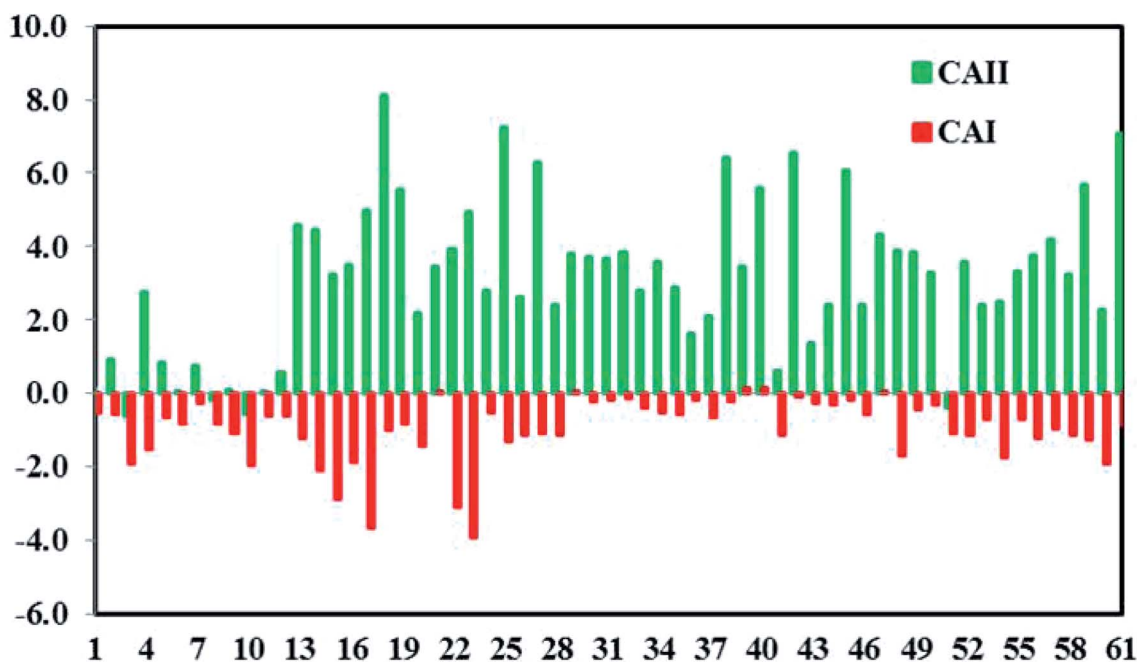
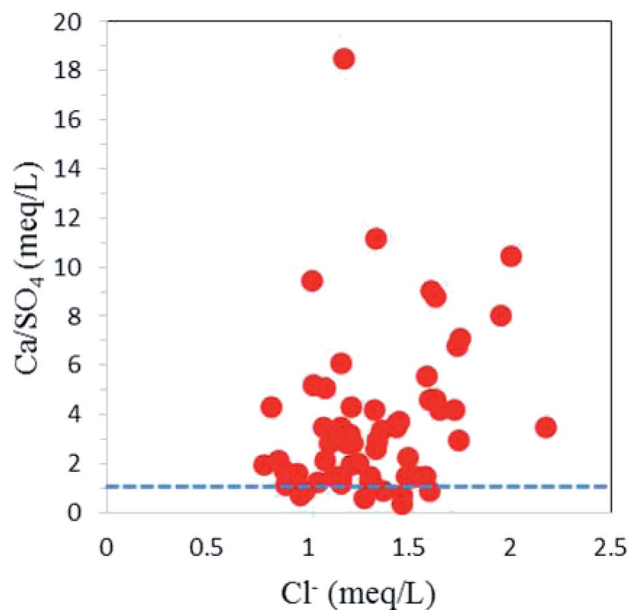Fig. 8   Chloro-alkaline indices (CAI 1 and CAI 2) indicating positive and reverse ion exchange processes.

Fig. 10   A scatter plot representing gypsum dissolution in the study area.

$$HQ_{Intake} = \frac{ADD_{In}}{RfD} \quad (11)$$

$$HQ_{dermal} = \frac{ADD_{De}}{RfD} \quad (12)$$

where ADD_{intake} and ADD_{dermal} represent the average daily dose for intake and dermal contact (mg per kg per day), C is the concentration of fluoride, EF is the exposure frequency (days per years), ED is exposure duration (years), BW is body weight (kg), AT is average time (days per years), CF is the conversion factor (l cm^{-3}), ESA is the exposed skin area (cm^2), and RfD indicates the reference dosage of fluoride content (0.06 mg per kg per day).

4.   Results and discussion

4.1   Hydrogeochemical scenario

The groundwater samples have pH of 7.13–8.13, indicating a slightly alkaline nature. It, however, falls within the desirable limit of the WHO guidelines (Table 2). Electrical conductivity (EC) of 180–3040 μS cm^{-1} indicates the influence of geochemical processes like dissolution and ion exchange on groundwater chemistry.[50] Total dissolved solids (TDS) range between 126 mg l^{-1} and 2128 mg l^{-1} and about six samples (10% of total samples) have values above the desirable limit (>1500 mg l^{-1}).[51] These samples with higher TDS might cause stomach annoyance and heart sickness along with the formation of kidney stones.[24,52,53] Higher TDS in groundwater might be due to high evaporation as the study area has an arid to semi-arid climate and experiences very high temperatures during the summer months. The total hardness varies between 36 and 792 mg l^{-1} and 12 samples (20% of the samples) surpass the desirable limit (Table 2).

4.2   Alkalis vs. alkali earths

Maximum values of major cations follow the order: Na^+ > Ca^{2+} > K^+ > Mg^{2+} (Table 2). The abundance of alkalis (Na^+ and K^+) is greater than those of the alkali earths (Ca^{2+} and Mg^{2+}) (e.g., ref. 52). The groundwater has 20–300 mg l^{-1} of Na and some samples surpass the allowable limit (>200 mg l^{-1}, WHO, 2017).[32] Some samples also have K (5–100 mg l^{-1}) above the desirable limit (>10 mg l^{-1}). We observed higher levels of sodium in the subsurface water samples from the northern part of the study area, suggesting that they originate from human activities in addition to the dissolution of Na-bearing silicate minerals.[54] The dissolution of microcline and orthoclase present in the watershed rocks provided potassium. Calcium varies between 12.80 mg l^{-1} and 174.40 mg l^{-1} and the groundwater has 0.96–85.44 mg l^{-1} of magnesium. Both are within the desirable limits of the WHO standards. We observed higher values of calcium and magnesium in the central part of the study area. The dissolution of ferro-magnesium minerals, such as pyroxenes, amphiboles and biotite, possibly contributed magnesium and calcium to the groundwater.[55,56] Additionally, the carbonate dissolution may also have contributed these ions to groundwater.[50]

4.3   Weak acids vs. strong acids

The maximum values of anions follow the order: HCO_3^- > Cl^- > SO_4^{2-} > NO_3^-. The concentrations of weak acids (HCO_3^- and

Table 3   Pearson's bivariate correlation matrix of groundwater quality parameters in samples from a semi-arid basin of South India

|	pH	EC	TDS	TH	Ca^{2+}	Mg^{2+}	Na^+	K^+	HCO_3^-	Cl^-	SO_4^{2-}	NO_3^-	PO_4^-
pH	1.00												
EC	0.09	1.00											
TDS	0.09	1.00	1.00										
TH	0.10	**0.96**	**0.96**	1.00									
Ca^{2+}	0.07	**0.96**	**0.96**	**0.99**	1.00								
Mg^{2+}	0.13	**0.95**	**0.95**	**0.99**	**0.96**	1.00							
Na^+	0.11	**0.97**	**0.97**	0.88	0.88	0.86	1.00						
K^+	0.07	**0.92**	**0.92**	0.87	0.86	0.86	**0.92**	1.00					
HCO_3^-	0.15	0.73	0.73	0.62	0.62	0.60	0.81	0.65	1.00				
Cl^-	0.00	0.86	0.86	0.82	0.82	0.80	0.83	0.87	0.37	1.00			
SO_4^{2-}	0.19	0.85	0.85	**0.91**	**0.90**	**0.91**	0.77	0.78	0.59	0.65	1.00		
NO_3^-	0.17	0.87	0.87	0.85	0.84	0.85	0.86	0.86	0.77	0.64	0.81	1.00	
PO_4^-	0.05	0.15	0.15	0.14	0.11	0.17	0.15	0.16	0.18	0.07	0.13	0.15	1.00
F^-	−0.08	0.47	0.47	0.39	0.40	0.37	0.52	0.44	0.48	0.39	0.33	0.38	−0.16
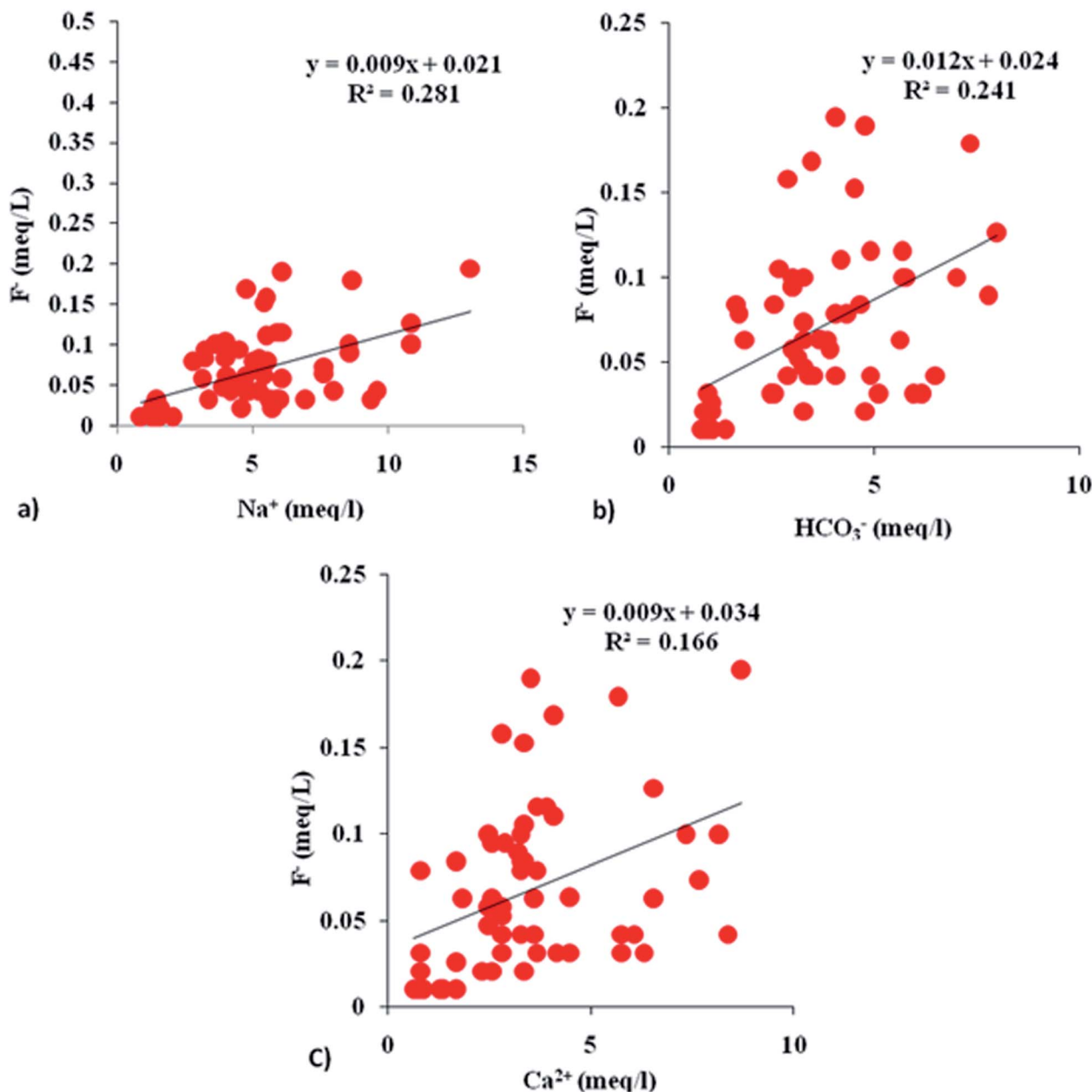
Fig. 11 Interionic plots (a–c) showing F^- vs. Na^+, HCO_3^- and Ca^{2+}.

CO_3^{2-}) are greater than those for the strong acids (Cl^-, SO_4^{2-} and NO_3^-).[52] Bicarbonate is the dominant anion (48–488 mg l^{-1}) followed by chloride (12–656 mg l^{-1}) and both have concentrations within the WHO limits.[51] Higher Cl compared to the desirable limit in one sample in the western part of the study area could be owing to domestic influences in the topsoil, as well as the semi-arid conditions of the study region.[57] The sulfate (21–395 mg l^{-1}) content is within the desirable limits. The phosphate concentrations (0.01–2.90 mg l^{-1}) of some of the samples are above the desirable limit (>0.3 mg l^{-1}, WHO, 2017). Nitrate (6–75 mg l^{-1}) in 13 samples remained above the desirable limit for WHO guidelines.[32]

4.4 Groundwater types

The Piper trilinear diagram[58] characterizes around 72.1% of the samples as mixed type (Ca^{2+}–Mg^{2+}–Cl^-), representing the transition from freshwater to brackish water (Fig. 2). Another 16.4% of them are of brackish Na–Cl water. About 8.2% of the samples are of Ca–Mg–SO_4 type and 3.3% fall in the field of Ca–Mg–HCO_3 water. In the modified diagram proposed by ref. 59, about 41% of the samples fall in the field representing strong acidic anions exceeding weak acidic anions (Fig. 3). Another 14.5% of the samples have more alkaline earths compared to alkali metals (i.e., Ca–Mg–Cl type), suggesting reverse ion exchange.

Table 4 The ranking and classification of groundwater samples for drinking as per EWQI

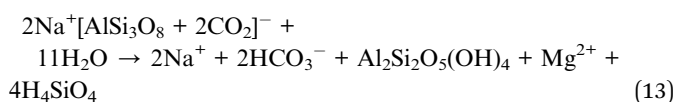| Sample no.	EWQI value	EWQI quality rank	Water quality
SRB-1	24.7	1	Excellent
SRB-2	41.4	2	Good
SRB-3	23.6	1	Excellent
SRB-4	69.3	3	Moderate
SRB-5	34.4	2	Good
SRB-6	24.3	1	Excellent
SRB-7	29.8	2	Good
SRB-8	26.4	2	Good
SRB-9	23.5	1	Excellent
SRB-10	18.8	1	Excellent
SRB-11	23.5	1	Excellent
SRB-12	34.3	2	Good
SRB-13	102.4	4	Poor
SRB-14	87.8	3	Moderate
SRB-15	75.7	3	Moderate
SRB-16	77.9	3	Moderate
SRB-17	100.8	4	Poor
SRB-18	155.8	5	Extremely poor
SRB-19	123.2	4	Poor
SRB-20	58.7	3	Moderate
SRB-21	87.8	3	Moderate
SRB-22	79.5	3	Moderate
SRB-23	87.0	3	Moderate
SRB-24	65.6	3	Moderate
SRB-25	143.6	4	Poor
SRB-26	70.0	3	Moderate
SRB-27	131.1	4	Poor
SRB-28	67.6	3	Moderate
SRB-29	145.2	4	Poor
SRB-30	137.2	4	Poor
SRB-31	96.6	3	Moderate
SRB-32	117.5	4	Poor
SRB-33	72	3	Moderate
SRB-34	79.7	3	Moderate
SRB-35	71.7	3	Moderate
SRB-36	53.5	3	Moderate
SRB-37	57	3	Moderate
SRB-38	133.8	4	Poor
SRB-39	91.3	3	Moderate
SRB-40	211.2	5	Extremely poor
SRB-41	33.5	2	Good
SRB-42	160.8	5	Extremely poor
SRB-43	56.4	3	Moderate
SRB-44	81.6	3	Moderate
SRB-45	155.6	5	Extremely poor
SRB-46	71.3	3	Moderate
SRB-47	105.1	4	Poor
SRB-48	83.4	3	Moderate
SRB-49	106.6	4	Poor
SRB-50	75.2	3	Moderate
SRB-51	38.1	2	Good
SRB-52	84.8	3	Moderate
SRB-53	71	3	Moderate
SRB-54	60.9	3	Moderate
SRB-55	87.6	3	Moderate
SRB-56	85.6	3	Moderate
SRB-57	102.9	4	Poor
SRB-58	75.8	3	Moderate
SRB-59	100.6	4	Poor
SRB-60	63.8	3	Moderate
SRB-61	138.9	4	Poor

4.5 Fluoride distribution

The IDW interpolation technique in ArcGIS (v.10.2.1) generated a spatial variation map for fluoride (0.2–3.7 mg l^{-1}) in the groundwater samples (Fig. 4). It divided the study area into four different regions with fluoride concentrations of <1 mg l^{-1}, 1–1.5 mg l^{-1}, 1.5–3 mg l^{-1} and >3 mg l^{-1}. About 44% of the total samples have <1 mg l^{-1}, 20% have 1–1.5 mg l^{-1}, 28% have 1.5–3 mg l^{-1} and 8% have more than 3 mg l^{-1} of fluoride. It was observed that >3 mg l^{-1} of fluoride was found in samples collected from five villages, namely Perumal pudur pirivu (3.4 mg l^{-1}), Tumbalpatti (3.2 mg l^{-1}), Andinaickenvalasu (3.7 mg l^{-1}), Narikkalpatti (3.0 mg l^{-1}) and Kondappanaick-enpatti (3.6 mg l^{-1}). A total of 22 villages in the study area have fluoride concentrations surpassing the WHO guidelines (>1.5 mg l^{-1}). All these villages with fluoride concentrations surpassing the WHO guidelines face the potential risks of dental fluorosis and skeletal fluorosis as well as skeletal cancer and neurotoxicological effects.[20,25,60–62] It has been suggested that the higher fluoride in groundwater could be due to rock weathering processes, deposition of atmospheric volcanic particles, agricultural runoff water and industrial effluents.

4.6 Hydrogeochemical control

The Gibbs diagrams[63] in Fig. 5 predict the factors responsible for the geochemical characteristics of the groundwater. A majority of the samples are grouped in the rock dominance field with just a few samples representing evaporation dominance. Generally, the warmer conditions, alkaline pH and rock weathering influence the water chemistry.[20,64] The rock weathering might have some influence and the groundwater chemistry in our study area is also influenced by temperature and uneven precipitation.

4.7 Silicate weathering

The rock weathering processes involve the alteration of silicate- and carbonate-bearing lithologies. The alteration of albite might be the source of excess Na^+ over Cl^- as per eqn (13).

$$2Na^+[AlSi_3O_8 + 2CO_2]^- + 11H_2O \rightarrow 2Na^+ + 2HCO_3^- + Al_2Si_2O_5(OH)_4 + Mg^{2+} + 4H_4SiO_4 \tag{13}$$

The concentration of Na^+ (meq l^{-1}) *versus* Cl^- (meq l^{-1}) was plotted to understand the influence of silicate weathering (Fig. 6a). Around 84% of the samples lie below the 1 : 1 line and they probably have a higher effect from anthropogenic activities along with minor silicate weathering. Most of the groundwater samples lie above the equiline (1 : 1) in the interionic plot of $Ca^{2+} + Mg^{2+}$ *versus* HCO_3^- (Fig. 6b). The excess Ca^{2+} and Mg^{2+} might react with Cl^- to materialise non-carbonate salts, such as $CaCl_2$ or $MgCl_2$.[65] Thus, silicate weathering is not the prime factor for higher Na^+ and HCO_3^- ions. Both of them might have originated from ion exchange processes.

Table 5 The number and percentage of groundwater samples in different EWQI drinking water categories

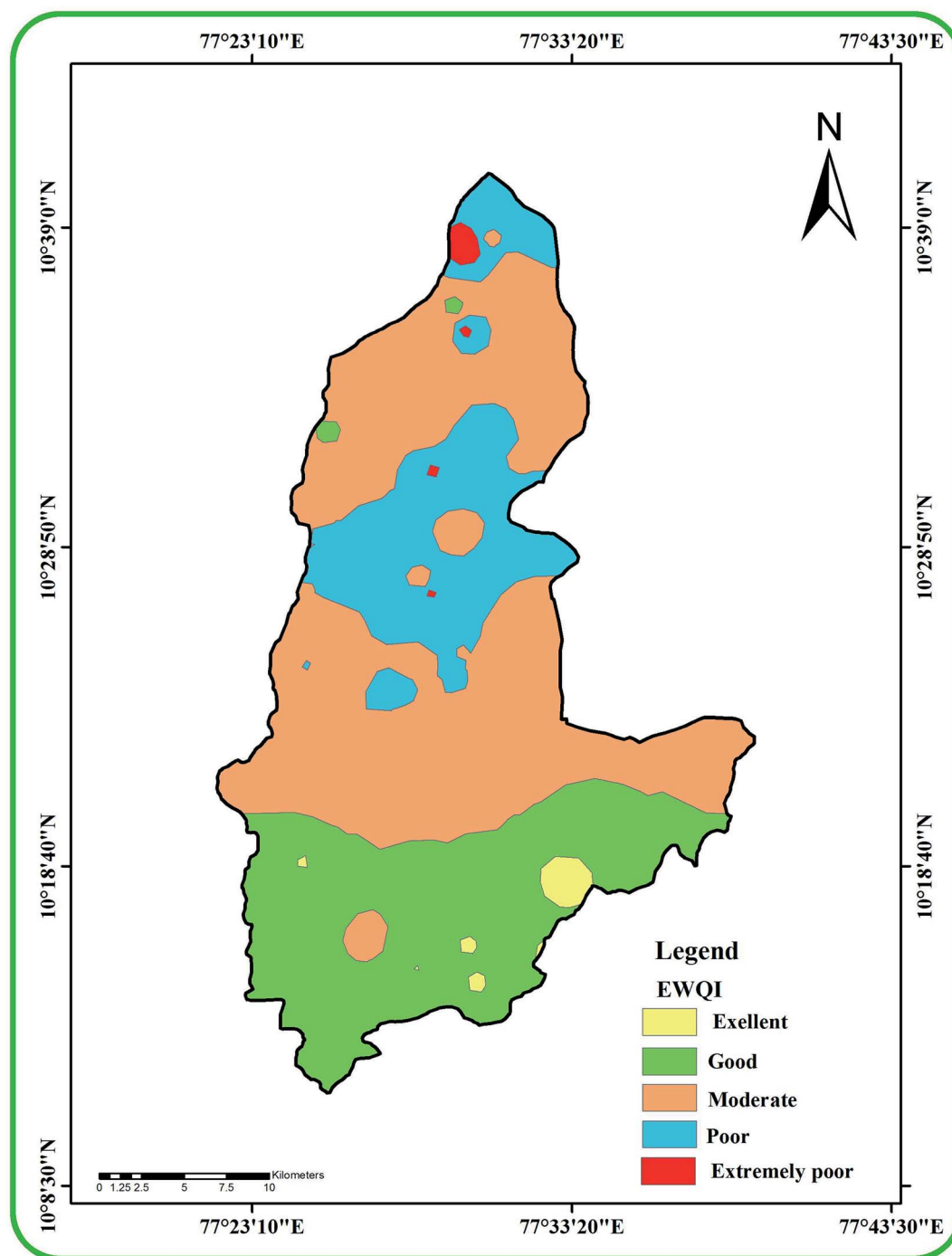| EWQI	<25	25–50	50–100	100–150	>150
Rank	1	2	3	4	5
No. of samples	6	7	30	14	4
%	9.84	11.48	49.18	22.95	6.55
Water quality	Excellent	Good	Moderate	Poor	Extremely poor

Fig. 12 A map showing the spatial distribution of groundwater quality classes in the study area based on EWQI.

Table 6   Hazard quotients (HQ) for different age groups based on fluoride ingestion in the study area

Sl. No	5 to 12 months	5 to 13 years	14 to 16 years	17 to 20 years	21 to 23 years	≥23 years	>65 years
SRB-1	0.36	0.15	0.11	0.08	0.11	0.12	0.11
SRB-2	0.73	0.31	0.22	0.18	0.23	0.24	0.22
SRB-3	0.36	0.15	0.11	0.09	0.11	0.12	0.11
SRB-4	1.82	0.78	0.56	0.43	0.58	0.62	0.56
SRB-5	0.36	0.15	0.11	0.09	0.11	0.12	0.11
SRB-6	0.36	0.15	0.11	0.09	0.11	0.12	0.11
SRB-7	0.36	0.15	0.11	0.08	0.11	0.12	0.11
SRB-8	1.09	0.46	0.33	0.26	0.34	0.37	0.34
SRB-9	0.73	0.31	0.22	0.18	0.23	0.24	0.22
SRB-10	0.36	0.15	0.11	0.09	0.11	0.12	0.11
SRB-11	0.36	0.15	0.11	0.09	0.11	0.12	0.11
SRB-12	0.36	0.15	0.11	0.09	0.11	0.12	0.11
SRB-13	4.09	1.71	1.23	0.96	1.27	1.36	1.25
SRB-14	0.73	0.31	0.22	0.17	0.23	0.24	0.22
SRB-15	1.45	0.62	0.44	0.35	0.46	0.49	0.45
SRB-16	1.45	0.62	0.44	0.35	0.46	0.49	0.45
SRB-17	4.02	1.71	1.23	0.96	1.26	1.36	1.25
SRB-18	4.36	1.87	1.34	1.05	1.38	1.49	1.36
SRB-19	1.09	0.46	0.33	0.26	0.34	0.37	0.34
SRB-20	2.05	0.85	0.61	0.48	0.63	0.68	0.62
SRB-21	1.09	0.46	0.33	0.26	0.34	0.37	0.34
SRB-22	2.18	0.93	0.67	0.52	0.69	0.74	0.68
SRB-23	1.09	0.46	0.33	0.26	0.34	0.37	0.34
SRB-24	0.73	0.31	0.22	0.17	0.23	0.24	0.22
SRB-25	6.27	2.65	1.90	1.49	1.96	2.11	1.93
SRB-26	3.40	1.48	1.06	0.83	1.09	1.18	1.08
SRB-27	1.45	0.62	0.44	0.35	0.46	0.49	0.45
SRB-28	2.90	1.24	0.89	0.70	0.92	0.99	0.91
SRB-29	1.45	0.62	0.44	0.35	0.46	0.49	0.45
SRB-30	2.54	1.09	0.78	0.61	0.80	0.87	0.79
SRB-31	5.81	2.49	1.79	1.40	1.84	1.99	1.82
SRB-32	2.18	0.93	0.67	0.52	0.69	0.74	0.68
SRB-33	3.40	1.48	1.06	0.83	1.09	1.18	1.08
SRB-34	2.18	0.93	0.67	0.52	0.69	0.74	0.68
SRB-35	2.05	0.85	0.61	0.48	0.63	0.68	0.62
SRB-36	2.18	0.93	0.67	0.52	0.69	0.74	0.68
SRB-37	1.09	0.46	0.33	0.26	0.34	0.37	0.34
SRB-38	1.09	0.46	0.33	0.26	0.34	0.37	0.34
SRB-39	1.09	0.46	0.33	0.26	0.34	0.37	0.34
SRB-40	6.77	2.88	2.07	1.62	2.13	2.30	2.10
SRB-41	0.96	0.39	0.28	0.21	0.28	0.31	0.28
SRB-42	3.40	1.48	1.06	0.83	1.09	1.18	1.08
SRB-43	2.90	1.24	0.89	0.70	0.92	0.99	0.91
SRB-44	5.45	2.34	1.67	1.31	1.73	1.86	1.70
SRB-45	3.40	1.48	1.06	0.83	1.09	1.18	1.08
SRB-46	3.63	1.56	1.11	0.87	1.15	1.24	1.13
SRB-47	2.26	0.94	0.67	0.53	0.69	0.75	0.69
SRB-48	2.90	1.24	0.89	0.70	0.92	0.99	0.91
SRB-49	1.45	0.62	0.44	0.35	0.46	0.49	0.45
SRB-50	1.45	0.62	0.44	0.35	0.46	0.49	0.45
SRB-51	2.77	1.17	0.83	0.65	0.86	0.93	0.85
SRB-52	3.86	1.63	1.17	0.92	1.21	1.30	1.19
SRB-53	3.27	1.40	1.00	0.79	1.03	1.11	1.02
SRB-54	1.68	0.70	0.50	0.39	0.51	0.56	0.51
SRB-55	5.31	2.26	1.62	1.27	1.67	1.80	1.64
SRB-56	2.77	1.17	0.83	0.65	0.86	0.93	0.85
SRB-57	6.53	2.80	2.01	1.58	2.07	2.23	2.04
SRB-58	2.77	1.17	0.83	0.65	0.86	0.93	0.85
SRB-59	3.14	1.32	0.95	0.74	0.98	1.06	0.96
SRB-60	3.27	1.40	1.00	0.79	1.03	1.12	1.02
SRB-61	3.40	1.48	1.06	0.83	1.09	1.18	1.08
Min.	**0.36**	**0.15**	**0.11**	**0.09**	**0.11**	**0.12**	**0.11**

Table 6 (Contd.)

Sl. No	5 to 12 months	5 to 13 years	14 to 16 years	17 to 20 years	21 to 23 years	≥23 years	>65 years
Max.	6.77	2.88	2.07	1.62	2.13	2.30	2.10
Mean	2.32	1.01	0.72	0.57	0.74	0.80	0.74

4.8 Ion exchange

The deficiency in Ca^{2+} + Mg^{2+} in 88.5% of the samples (Na^+/Cl^- ratio > 1) confirms the contribution of cation exchange to the groundwater geochemistry.[66] Both the Ca^{2+} and Mg^{2+} get adsorbed on exchangeable sites of clay minerals, and simultaneously Na^+ is released. This ion exchange process reduces the concentrations of Ca^{2+} and Mg^{2+} and increases the Na^+ concentration in the groundwater samples. The scatter plot of Ca^{2+}–Mg^{2+}–SO_4^{2-}–HCO_3^- versus Na^+–Cl^- confirms the role of ion exchange processes (Fig. 7). Sampling points near the straight line with a slope of −1 indicate the existence of ion exchange.[67] The majority of samples being in the reverse ion exchange zone strongly supports the dominant influence of reverse ion exchange in the study region. Some samples close to zero on the Na^+–Cl^- axis are unaffected by ion exchange.

Chloro-alkaline indices (CAI) 1 and 2 from ref. 68 were used to identify the controlling factors responsible for the ion exchange processes.[50,69] CAI 1 and CAI 2 were calculated using eqn (14) and (15) and considering all of the ions as meq l^{-1}.

$$CAI\ 1 = Cl^- - (Na^+ + K^+)/Cl^- \tag{14}$$

$$CAI\ 2 = Cl^- - (Na^+ + K^+)/SO_4^{2-} + HCO_3^- + CO_3^- + NO_3^- \tag{15}$$

Negative CAI values in 87% of the samples support that reverse ion exchange is a major hydrogeochemical process that controls the groundwater chemistry (Fig. 8). The exchange of sodium and potassium in water with calcium and magnesium in host rocks yielded a negative value of CAI.

4.9 Carbonate and sulfate dissolution

Around 85% of sampling points fall on the 1 : 1 line of Ca^{2+} + Mg^{2+} versus HCO_3^- + SO_4^{2-} scatter plot with HCO_3^- + SO_4^{2-} < 10 meq l^{-1}, suggesting calcite dissolution (Fig. 9). The dominance of calcite dissolution is further confirmed by the Ca^{2+}/Mg^{2+} molar ratio.[20] All the groundwater samples have Ca^{2+}/Mg^{2+} molar ratios of more than, which signifies the dominance of calcite dissolution over dolomite dissolution by reverse ion exchange. The high calcium- and sulfate-bearing groundwater is also attributed to gypsum ($CaSO_4 \cdot 2H_2O$) dissolution. The samples (about 15% of all samples) with HCO_3^- + SO_4^{2-} > 10 meq l^{-1} on the scatter plot Ca^{2+} + Mg^{2+} versus HCO_3^- + SO_4^{2-} were affected by the gypsum dissolution. Most of the samples falling above the unity line of Ca^{2+}/SO_4^{2-} molar ratio versus Cl^- (meq l^{-1}) plot had minimal influence from gypsum dissolution (Fig. 10).

4.10 Fluoride dissolution

Fluoride content lacks any correlation ($r = -0.1$) with the pH (Table 3). The positive correlation between F^- and HCO_3^- ($r =$ 0.5), however, confirms the coexistence of calcite and fluorite dissolution. The HCO_3^--enriched groundwater (alkaline conditions) facilitated the dissolution of CaF_2 and thus increased the F^- concentration. The positive correlations between F^- and Ca^{2+} ($r = 0.4$) and F^- and Mg^{2+} ($r = 0.4$) indicate that the dissolution of both CaF_2 and MgF_2 contributed fluoride to the groundwater.[20] Dissolution of the fluorite- and fluoride-rich silicates is also supported by the positive correlation ($r = 0.5$) between Na^+ and F^-. Comparable R^2 values between Na^+ and F^- as well as between HCO_3^- and F^- in the interionic plot show that the high F^- concentrations in groundwater samples were contributed by fluoride-rich silicates as well as calcite (Fig. 11a and b).[20,70] The relatively lower influence of CaF_2 is supported by lower positive correlation values between F^- and Ca^{2+} (Fig. 11c).

4.11 Anthropogenic source

The relationship between ions and the TDS was used as an indicator for anthropogenic factors, such as chemical fertilizers, infiltration of organic matter, synthetic fertilizers, runoff from the surrounding agricultural fields, and wastewater effluents. Strong positive correlations of TDS with different cations Ca^{2+} ($r = 0.9$), Mg^{2+} ($r = 0.9$), Na^+ ($r = 0.9$) and K^+ ($r = 0.9$) confirm the contributions from anthropogenic activities in addition to contributions of geogenic origin these cations. Equally stronger positive correlations of TDS with anions Cl^- ($r = 0.9$), SO_4^{2-} ($r = 0.8$), NO_3^- ($r = 0.9$) and F^- ($r = 0.5$) also suggest the influence of anthropogenic activities. The positive correlation between NO_3^- and F^- indicates that F^- also partly comes from anthropogenic sources such as fertilizers. The application of phosphate fertilizer might be one of the anthropogenic sources of fluoride in the study area. The minor negative correlation between F^- and PO_4^- ($r = -0.2$), however, ruled out the possibility that a large part of the fluoride in the groundwater is from phosphate fertilizers.[71]

4.12 EWQI-based groundwater quality

EWQI values were calculated using the hydro-chemical parameters and the quality ranking of groundwater samples is presented in Table 4. Water samples with EWQI < 100 are suitable for drinking while samples with EWQI > 100 are not suitable for drinking. This model characterizes sample 10 in the study area as less polluted (EWQI: 18.8) and sample 40 as highly polluted (EWQI: 211.3). Table 5 presents the number and percentage of samples in each of the EWQI quality ranking groups. Six samples (9.9%) are classified as excellent, seven samples (11.5%) are ranked as good and 30 samples (49.2%) are in the moderate category. The 14 poor samples (23%) and four extremely poor samples (6.6%) are not acceptable for drinking (Fig. 12). Samples in the extremely poor

Table 7 Hazard quotients (HQ) for different age groups based on the dermal pathway of fluoride in the study area

Sl. no	5 to 12 months	5 to 13 years	14 to 16 years	17 to 20 years	21 to 23 years	≥23 years	>65 years
SRB-1	0.002	0.001	0.001	0.000	0.001	0.001	0.001
SRB-2	0.003	0.002	0.002	0.000	0.002	0.002	0.002
SRB-3	0.002	0.001	0.001	0.000	0.001	0.001	0.001
SRB-4	0.008	0.006	0.005	0.001	0.005	0.004	0.004
SRB-5	0.002	0.001	0.001	0.000	0.001	0.001	0.001
SRB-6	0.002	0.001	0.001	0.000	0.001	0.001	0.001
SRB-7	0.002	0.001	0.001	0.000	0.001	0.001	0.001
SRB-8	0.005	0.003	0.003	0.001	0.003	0.002	0.002
SRB-9	0.003	0.002	0.002	0.000	0.002	0.002	0.002
SRB-10	0.002	0.001	0.001	0.000	0.001	0.001	0.001
SRB-11	0.002	0.001	0.001	0.000	0.001	0.001	0.001
SRB-12	0.002	0.001	0.001	0.000	0.001	0.001	0.001
SRB-13	0.017	0.013	0.010	0.002	0.010	0.009	0.009
SRB-14	0.003	0.002	0.002	0.000	0.002	0.002	0.002
SRB-15	0.006	0.005	0.004	0.001	0.004	0.003	0.003
SRB-16	0.006	0.005	0.004	0.001	0.004	0.003	0.003
SRB-17	0.017	0.013	0.010	0.002	0.010	0.009	0.009
SRB-18	0.019	0.014	0.011	0.002	0.011	0.010	0.009
SRB-19	0.005	0.003	0.003	0.001	0.003	0.002	0.002
SRB-20	0.009	0.006	0.005	0.001	0.005	0.004	0.004
SRB-21	0.005	0.003	0.003	0.001	0.003	0.002	0.002
SRB-22	0.009	0.007	0.006	0.001	0.006	0.005	0.005
SRB-23	0.005	0.003	0.003	0.001	0.003	0.002	0.002
SRB-24	0.003	0.002	0.002	0.000	0.002	0.002	0.002
SRB-25	0.027	0.019	0.016	0.003	0.016	0.014	0.013
SRB-26	0.015	0.011	0.009	0.002	0.009	0.008	0.007
SRB-27	0.006	0.005	0.004	0.001	0.004	0.003	0.003
SRB-28	0.013	0.009	0.007	0.001	0.007	0.006	0.006
SRB-29	0.006	0.005	0.004	0.001	0.004	0.003	0.003
SRB-30	0.011	0.008	0.006	0.001	0.006	0.006	0.005
SRB-31	0.025	0.018	0.015	0.003	0.015	0.013	0.012
SRB-32	0.009	0.007	0.006	0.001	0.006	0.005	0.005
SRB-33	0.015	0.011	0.009	0.002	0.009	0.008	0.007
SRB-34	0.009	0.007	0.006	0.001	0.006	0.005	0.005
SRB-35	0.009	0.006	0.005	0.001	0.005	0.004	0.004
SRB-36	0.009	0.007	0.006	0.001	0.006	0.005	0.005
SRB-37	0.005	0.003	0.003	0.001	0.003	0.002	0.002
SRB-38	0.005	0.003	0.003	0.001	0.003	0.002	0.002
SRB-39	0.005	0.003	0.003	0.001	0.003	0.002	0.002
SRB-40	0.029	0.021	0.017	0.003	0.017	0.015	0.014
SRB-41	0.004	0.003	0.002	0.000	0.002	0.002	0.002
SRB-42	0.015	0.011	0.009	0.002	0.009	0.008	0.007
SRB-43	0.013	0.009	0.007	0.001	0.007	0.006	0.006
SRB-44	0.024	0.017	0.014	0.003	0.014	0.012	0.012
SRB-45	0.015	0.011	0.009	0.002	0.009	0.008	0.007
SRB-46	0.016	0.011	0.009	0.002	0.009	0.008	0.008
SRB-47	0.010	0.007	0.006	0.001	0.006	0.005	0.005
SRB-48	0.013	0.009	0.007	0.001	0.007	0.006	0.006
SRB-49	0.006	0.005	0.004	0.001	0.004	0.003	0.003
SRB-50	0.006	0.005	0.004	0.001	0.004	0.003	0.003
SRB-51	0.012	0.009	0.007	0.001	0.007	0.006	0.006
SRB-52	0.017	0.012	0.010	0.002	0.010	0.008	0.008
SRB-53	0.014	0.010	0.008	0.002	0.008	0.007	0.007
SRB-54	0.007	0.005	0.004	0.001	0.004	0.004	0.003
SRB-55	0.023	0.017	0.013	0.002	0.013	0.012	0.011
SRB-56	0.012	0.009	0.007	0.001	0.007	0.006	0.006
SRB-57	0.028	0.021	0.017	0.003	0.017	0.014	0.014
SRB-58	0.012	0.009	0.007	0.001	0.007	0.006	0.006
SRB-59	0.013	0.010	0.008	0.001	0.008	0.007	0.007
SRB-60	0.014	0.010	0.008	0.002	0.008	0.007	0.007
SRB-61	0.015	0.011	0.009	0.002	0.009	0.008	0.007
Min.	**0.002**	**0.001**	**0.001**	**0.000**	**0.001**	**0.001**	**0.001**
Max.	**0.029**	**0.021**	**0.017**	**0.003**	**0.017**	**0.015**	**0.014**
Mean	**0.010**	**0.007**	**0.006**	**0.001**	**0.006**	**0.005**	**0.005**

Table 8 Total hazard indices for different age groups in the study area

Sl. no	5 to 12 months	5 to 13 years	14 to 16 years	17 to 20 years	21 to 23 years	≥23 years	> 65 years
SRB-1	0.36	0.15	0.11	0.09	0.11	0.12	0.11
SRB-2	0.73	0.31	0.22	0.17	0.23	0.25	0.23
SRB-3	0.36	0.15	0.11	0.09	0.11	0.12	0.11
SRB-4	1.83	0.78	0.56	0.44	0.57	0.62	0.57
SRB-5	0.36	0.15	0.11	0.08	0.11	0.12	0.11
SRB-6	0.36	0.15	0.11	0.08	0.11	0.12	0.11
SRB-7	0.36	0.15	0.11	0.08	0.11	0.12	0.11
SRB-8	1.10	0.47	0.33	0.26	0.34	0.37	0.34
SRB-9	0.73	0.31	0.22	0.17	0.23	0.25	0.22
SRB-10	0.36	0.15	0.11	0.08	0.11	0.12	0.11
SRB-11	0.36	0.15	0.11	0.08	0.11	0.12	0.11
SRB-12	0.36	0.15	0.11	0.08	0.11	0.12	0.11
SRB-13	4.04	1.72	1.24	0.96	1.27	1.37	1.26
SRB-14	0.73	0.31	0.22	0.17	0.23	0.25	0.22
SRB-15	1.47	0.62	0.45	0.35	0.46	0.50	0.45
SRB-16	1.47	0.62	0.45	0.35	0.46	0.50	0.45
SRB-17	4.04	1.72	1.24	0.96	1.27	1.37	1.26
SRB-18	4.41	1.88	1.35	1.05	1.38	1.50	1.37
SRB-19	1.10	0.47	0.33	0.26	0.34	0.37	0.34
SRB-20	2.02	0.86	0.62	0.48	0.63	0.68	0.63
SRB-21	1.10	0.47	0.33	0.26	0.34	0.37	0.34
SRB-22	2.20	0.94	0.67	0.52	0.69	0.75	0.68
SRB-23	1.10	0.47	0.33	0.26	0.34	0.37	0.34
SRB-24	0.73	0.31	0.22	0.17	0.23	0.25	0.23
SRB-25	6.25	2.67	1.91	1.49	1.96	2.12	1.95
SRB-26	3.49	1.49	1.07	0.83	1.09	1.19	1.09
SRB-27	1.47	0.63	0.45	0.35	0.46	0.50	0.46
SRB-28	2.94	1.25	0.90	0.70	0.92	1.00	0.92
SRB-29	1.47	0.63	0.45	0.35	0.46	0.50	0.46
SRB-30	2.57	1.10	0.79	0.61	0.80	0.87	0.80
SRB-31	5.88	2.51	1.80	1.40	1.84	2.00	1.83
SRB-32	2.20	0.94	0.67	0.52	0.69	0.75	0.68
SRB-33	3.49	1.49	1.07	0.83	1.09	1.19	1.08
SRB-34	2.20	0.94	0.67	0.52	0.69	0.75	0.68
SRB-35	2.02	0.86	0.62	0.48	0.63	0.69	0.630
SRB-36	2.20	0.94	0.67	0.52	0.69	0.75	0.68
SRB-37	1.10	0.47	0.33	0.26	0.34	0.37	0.34
SRB-38	1.10	0.47	0.33	0.26	0.34	0.37	0.34
SRB-39	1.10	0.47	0.33	0.26	0.34	0.37	0.34
SRB-40	6.80	2.90	2.08	1.62	2.19	2.31	2.11
SRB-41	0.92	0.39	0.28	0.22	0.29	0.31	0.28
SRB-42	3.49	1.49	1.07	0.83	1.20	1.18	1.08
SRB-43	2.94	1.25	0.90	0.70	0.92	1.00	0.91
SRB-44	5.51	2.35	1.69	1.31	1.73	1.87	1.71
SRB-45	3.49	1.49	1.07	0.83	1.20	1.18	1.08
SRB-46	3.67	1.57	1.12	0.87	1.15	1.25	1.14
SRB-47	2.22	0.95	0.68	0.53	0.70	0.75	0.69
SRB-48	2.94	1.25	0.90	0.70	0.92	1.00	0.91
SRB-49	1.47	0.62	0.45	0.35	0.46	0.50	0.45
SRB-50	1.47	0.62	0.45	0.35	0.46	0.50	0.45
SRB-51	2.75	1.17	0.84	0.66	0.86	0.93	0.85
SRB-52	3.86	1.65	1.18	0.92	1.21	1.31	1.20
SRB-53	3.31	1.41	1.01	0.79	1.04	1.12	1.03
SRB-54	1.65	0.70	0.50	0.39	0.52	0.56	0.51
SRB-55	5.33	2.27	1.63	1.27	1.67	1.81	1.66
SRB-56	2.75	1.17	0.84	0.66	0.86	0.93	0.85
SRB-57	6.62	2.82	2.03	1.58	2.08	2.25	2.06
SRB-58	2.75	1.17	0.84	0.66	0.86	0.93	0.85
SRB-59	3.12	1.33	0.95	0.74	0.98	1.06	0.97
SRB-60	3.31	1.41	1.01	0.79	1.04	1.12	1.03
SRB-61	3.49	1.49	1.07	0.83	1.09	1.18	1.08
% of risk	79%	43%	30%	11%	30%	36%	30%

quality category (18, 40, 42 and 45) have high loading of Na^+, Ca^{2+}, HCO_3^-, Cl^-, NO_3^- and F^- owing to the higher influence of anthropogenic inputs. Our study found that poor and extremely poor quality samples are present in the hornblende biotite gneiss lithologies (northern central part). The excellent to good categories of water exist under the charnockite rock (southern part). Our study indicates that lithology is an important reason for the variation in water quality. The arid or semi-arid condition (more evaporation) of this region is also another reason for the moderate to poor quality of the groundwater.

4.13   Human health risks from fluoride intake

A high amount of fluoride intake can cause health issues in humans. We identify the non-carcinogenic risks in populations in seven age groups: 5–12 months, 5–13 years, 14–16 years, 17–20 years, 21–23 years, ≥23 years and >65 years (Tables 6 and 7). The risk analysis was done for two routes of fluoride exposure: i.e. (i) intake of water and (ii) dermal contact of individuals. Table 8 presents the total hazard indices (THI) calculated for all these age groups.

4.14   Ingestion pathway

The hazard quotients for intake (ADD_{intake}) of high fluoride concentrations were assessed by integrating the pollutants obtained from the US EPA 2011 handbook as well as the fluoride variation in the groundwater of the study area. A similar estimation and the impact of fluoride contamination in the groundwater of southwestern Nigeria[53] and central Telangana state (India)[72] on human health were attempted. The hazard quotients ranged from 0.37 to 6.78 (5–12 months), 0.16 to 2.89 (5–13 years), 0.11 to 2.07 (14–16 years), 0.09 to 1.62 (17–20 years), 0.12 to 2.14 (21–23 years), 0.12 to 2.30 (≥23 years) and

0.114 to 2.104 (>65 years) for the different age groups (Table 6). The ADD_{intake} hazard quotients show that 79% of the samples exceeded the permissible limit (HQ = 1) for the 5–12 months age group, 43% of samples were above the permissible limit for the 5–13 years age group and 30% of the samples were above the acceptable limit for the 14–16 years population. The 5–12 months group is more prone to fluoride exposure owing to the consumption of groundwater. The remaining age groups of 17–20 years (11%), 21–23 years (30%), >23 years (31%) and >65 years (30%) are at risk from relatively lower numbers of water samples.

4.15   Dermal pathway

The calculated ADD_{dermal} hazard quotients varied from 0.002 to 0.029 (5–12 months), 0.001 to 0.021 (5–13 years), 0.001 to 0.017 (14–16 years), 0.000 to 0.003 (17–20 years), 0.001 to 0.017 (21–23 years), 0.001 to 0.015 (≥23 years) and 0.001 to 0.014 (>65 years) in the populations of different age groups (Table 7). Our results suggest that the ADD_{dermal} pathway poses less risk compared to the ADD_{intake} estimations.

4.16   Total hazard index (THI)

THI values higher than the permissible limit were found in 79% of the samples for the 5–12 months age group and about 43% of samples are unsuitable for the 5–13 years age group. The 14–16 years age group has a potential hazard from 30% of the samples (Fig. 13 and Table 8). The results of the non-carcinogenic health risk assessment designate the 5–12 months age group as the most likely to receive health hazards from the consumption of fluoride-contaminated drinking water. In the remaining age groups, THI values higher than the acceptable limit are
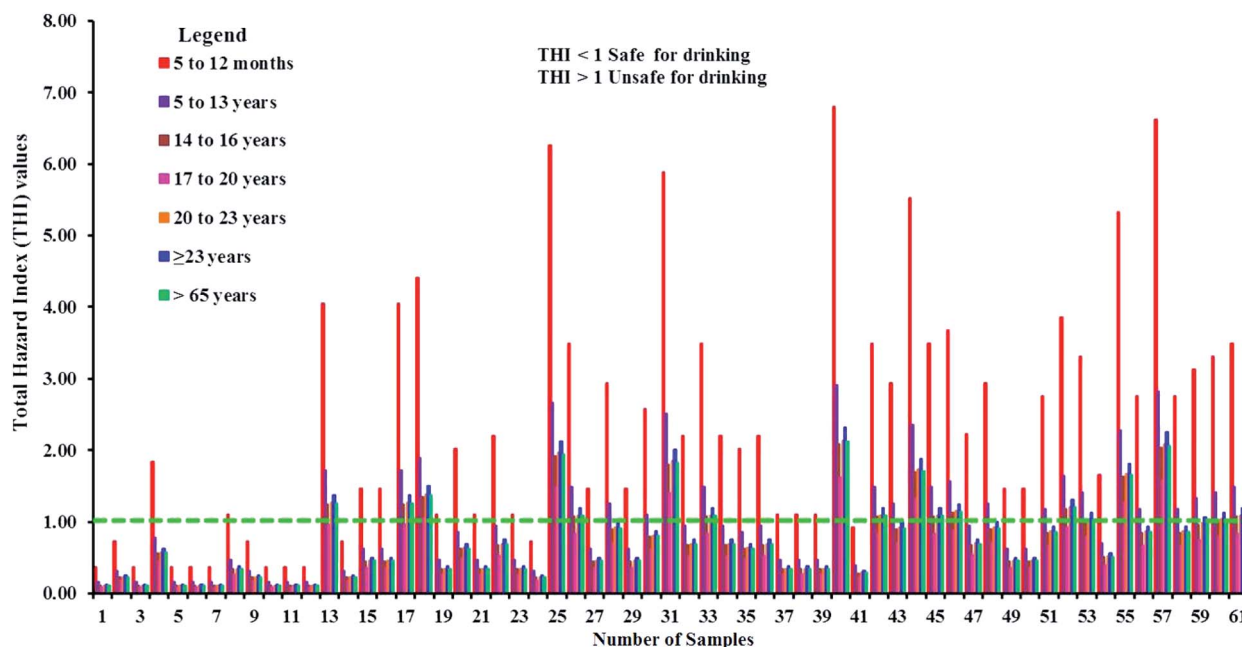

Fig. 13   Samples representing safe and risk categories among different age groups in the study area based on THI.

observed in 11% (17–20 years), 30% (21–23 years), 36% (≥23 years), and 30% (≥65 years) of the total samples, respectively.

5. Conclusions

In this work, 61 groundwater samples were collected and analyzed for different hydrogeochemical parameters to comprehend the geochemical processes affecting the fluoride contamination in the groundwater of a semi-arid part of South India. All these samples have more alkalis and strong acids compared to alkali earths and weak acids. Most of them are of mixed Ca–Mg–Cl type, followed by Na–Cl type water. Some of the important conclusions of this study are:

(i) Silicate weathering is not the prime factor for higher Na^+ and HCO_3^-. Deficiencies in $Ca^{2+} + Mg^{2+}$ confirm the contribution of cation exchange to the groundwater geochemistry.

(ii) Around 85% of sampling points fall on the 1 : 1 line of the $Ca^{2+} + Mg^{2+}$ versus $HCO_3^- + SO_4^{2-}$ scatter plot, suggesting the dominant influence of calcite dissolution and less influence from gypsum dissolution.

(iii) A total of 22 villages in the study area have fluoride concentrations surpassing the WHO guideline (>1.5 mg l^{-1}), and we observed >3 mg l^{-1} of fluoride in samples from five villages.

(iv) A large amount of the fluoride in groundwater is contributed by fluoride-rich silicates as well as calcite. CaF_2 also contributed a minor amount of fluoride. However, we ruled out the possibility that phosphate fertilizers contributed a large part of the fluoride present in the groundwater.

(v) EWQI values place about 30% of the samples in the poor and extremely poor categories. These samples have high loadings of Na^+, Ca^{2+}, HCO_3^-, Cl^-, NO_3^- and F^- owing to the higher influence of anthropogenic inputs. Most of them are from aquifers with hornblende biotite gneiss lithology (northern central part). Our study indicates that lithology is an important reason for variation in water quality, apart from the arid or semi-arid conditions (more evaporation) of this region.

(vi) ADD_{intake} hazard quotient analysis shows that the 5–12 month-old group is more prone to fluoride exposure owing to the consumption of groundwater. The remaining age groups of 17–20 years (11%), 21–23 years (30%), >23 years (31%) and >65 years (30%) are at risk from a relatively lower number of water samples.

(vii) The calculation of hazard quotients suggests that the dermal pathway (0.001–0.029) poses less health risk compared to the ingestion pathway (009–6.78). Long-term monitoring, checking on the disposal of domestic waste, and proper well lining are some of the crucial factors for maintaining proper health conditions in this region.

Conflicts of interest

The authors declare that they have no conflicts interests.

Acknowledgements

References

1 P. Li and J. Wu, Hum. Ecol. Risk Assess., 2019, 25(1–2), 1–10.

2 C. Qian, X. Wu, W. P. Mu, R. Z. Fu, G. Zhu, Z. R. Wang and D. D. Wang, Environ. Earth Sci., 2016, 75, 1356.

3 A. A. Mohammadi, M. Yousefi, J. Soltani, A. G. Ahangar and S. Javan, Environ. Sci. Pollut. Control Ser., 2018, 25, 30315–30324.

4 S. Duraisamy, V. Govindhaswamy, K. Duraisamy, S. Krishinaraj, A. Balasubramanian and S. Thirumalaisamy, Environ. Geochem. Health, 2018, 41, 851–873, DOI: 10.1007/s10653-018-0183-z.

5 M. Qasemi, M. Shams, S. A. Sajjadi, M. Farhang, S. Erfanpoor, M. Yousefi, A. Zarei and M. Afsharnia, Biol. Trace Elem. Res., 2019, 192, 106–115, DOI: 10.1007/s12011-019-1660-7.

6 S. L. Amaral, L. B. Azevedo, M. A. Buzalaf, M. F. Fabricio, M. S. Fernandes, R. A. Valentine, A. Maguire and F. V. Zohoori, Sci. Rep., 2018, 8, 3211.

7 M. Ghaderpoori, B. Kamarehie, A. Jafari, A. Ghaderpoury and M. A. Karami, Data in Brief, 2018, 16, 658–692.

8 S. He and J. Wu, Exposure Health, 2019, 11(2), 125–137, DOI: 10.1007/s12403-018-0289-7.

9 X. He, J. Wu and S. He, Hum. Ecol. Risk Assess., 2019, 25(1–2), 32–51.

10 J. Shen and A. I. Schafer, Sci. Total Environ., 2015, 527–528, 520–529.

11 M. Panneer, R. Sivakumar and M. Senthilkumar, Int. J. Environ. Sci. Technol., 2017, 14(9), 1931–1944, DOI: 10.1007/s13762-017-1277-3.

12 S. Satheeshkumar, S. Venkateswaran and R. Kannan, Acta Geochim., 2017, 36(1), 112–123, DOI: 10.1007/s11631-016-0137-z.

13 C. Thivya, S. Chidambaram, M. S. Rao, R. Thilagavathi, M. V. Prasanna and S. Manikandan, Appl. Water Sci., 2015, 7, 1011–1023, DOI: 10.1007/s13201-015-0312-0.

14 B. Xu, Y. Zhang and J. Wang, Hum. Ecol. Risk Assess., 2019, 1–20, DOI: 10.1080/10807039.2018.1530939.

15 G. C. Kisku and P. Sahu, Environmental Concerns and Sustainable Development, 2019, pp. 213–233.

16 N. S. Rao and M. Chaudhary, Groundwater for Sustainable Development, 2019b, 9, 100238.

17 S. Battaleb-Looie, F. Moore, H. Jafari, G. Jacks and D. Ozsvath, Environ. Earth Sci., 2012, 67(4), 1173–1182.

18 R. Dehbandi, F. Moore and B. Keshavarzi, Chemosphere, 2018, 193, 763–776.

19 I. Mukherjee and U. K. Singh, Environ. Geochem. Health, 2018, 40, 2259–2301, DOI: 10.1007/s10653-018-0096-x.

20 D. Marghade, D. B. Malpe, N. S. Rao and B. Sunitha, Hum. Ecol. Risk Assess., 2019, 1–22.

21 R. A. Fallahzadeh, M. Miri, M. Taghavi, A. Gholizadeh, R. Anbarani, A. Hosseini- Bandegharaei, M. Ferrante and G. O. Conti, Food Chem. Toxicol., 2018, 113, 314–321.

22 W. Guissouma, O. Hakami, A. J. Al-Rajab and J. Tarhouni, *Chemosphere*, 2017, **177**, 102–108.

23 S. P. S. Teotia and M. Teotia, *Fluoride*, 1994, **27**(2), 59–66.

24 P. Sahu, G. C. Kisku, P. K. Singh, V. Kumar, P. Kumar and N. Shukla, *Environ. Earth Sci.*, 2018, **77**, 484.

25 WHO, *Fluoride in drinking water*, World Health Organization, IWA Publication, London, 2006.

26 T. G. Kazi, K. D. Brahman, H. I. Afridi, F. Shah and M. B. Arain, *Environ. Sci. Pollut. Res.*, 2018, **25**(13), 12909–12914, DOI: 10.1007/s11356-018-1563-8.

27 J. Wu, H. Zhou, S. He and Y. Zhang, *Environ. Earth Sci.*, 2019, **78**(15), 446, DOI: 10.1007/s12665-019-8471-1.

28 K. K. Yadav, V. Kumar, S. Kumar, S. Rezania and N. Singh, *Regul. Toxicol. Pharmacol.*, 2019, **106**, 68–80, DOI: 10.1016/j.yrtph.2019.04.013.

29 N. Ranasinghe, E. Kruger and M. Tennant, *Int. Dent. J.*, 2019, **69**(4), 295–302, DOI: 10.1111/idj.12476.

30 M. Yousefi, M. Ghoochani and A. H. Mahvi, *Ecotoxicol. Environ. Saf.*, 2018, **148**, 426–430.

31 A. K. Susheela, *Proc. Indian Natl. Sci. Acad.*, 2002, **68B**(5), 389–400.

32 P. Li, H. Qian and J. Wu, *E-J. Chem.*, 2010, **7**(s1), S209–S216.

33 V. Amiri, M. Rezaei and N. Sohrabi, *Environ. Earth Sci.*, 2014, **72**(9), 3479.

34 D. Li, X. Gao, Y. Wang and W. Luo, *Environ. Pollut.*, 2018, **237**, 430–441.

35 A. D. Gorgij, J. Wu and A. A. Moghadam, *Hum. Ecol. Risk Assess.*, 2019, **25**(1–2), 176–190, DOI: 10.1080/10807039.2018.1564235.

36 J. Wu, P. Li, H. Qian and J. Chen, *Environ. Earth Sci.*, 2015, **74**(3), 2185–2195, DOI: 10.1007/s12665-015-4208.

37 L. Zhang, D. Huang, J. Yang, X. Wei, J. Qin, S. Ou, Z. Zhang and Y. Zou, *Environ. Pollut.*, 2017, **222**, 118–125, DOI: 10.1016/j.envpol.2016.12.074.

38 T. Walia, S. Abu Fanas, M. Akbar, J. Eddin and M. Adnan, *The Saudi Dental Journal*, 2017, **29**, 117–122, DOI: 10.1016/j.sdentj.2017.04.002.

39 M. Yousefi, S. Ghalehaskar, F. B. Asghari, A. Ghaderpoury, M. H. Dehghani, M. Ghaderpoori and A. A. Mohammadi, *Regul. Toxicol. Pharmacol.*, 2019, 104408, DOI: 10.1016/j.yrtph.2019.104408.

40 C. Thivya, S. Chidambaram, M. S. Rao, R. Thilagavathi, M. V. Prasanna and S. Manikandan, *Appl. Water Sci.*, 2017, **7**, 1011–1023.

41 Central Ground Water Board (CGWB), *District Groundwater Brochure*, Dindigul district, Tamil Nadu, 2008.

42 GSI, *Geological and mineral map of Tamil Nadu and Pondicherry*, 1995, Published by the Director General Geological Survey of India on 1: 500,000 scale.

43 APHA, AWWA and WPCF, *Standard methods for the examination of waters and waste waters*, American Public Health Association (APHA), Washington, 21st edn, 2005.

44 P. Li, X. Li, X. Meng, M. Li and Y. Zhang, *Exposure Health*, 2016, **8**(3), 361–379, DOI: 10.1007/s12403-016-0205-y.

45 Q. Guo, Y. Wang, T. Ma and R. Ma, *J. Geochem. Explor.*, 2007, **93**(1), 1–12.

46 USEPA, *Exposure Factors Handbook: 2011 Edition*, U.S. Environmental Protection Agency, 2011 edn, 2011, EPA/600/R-090/052F.

47 J. Wu and Z. Sun, *Exposure Health*, 2016, **8**(3), 311–329, DOI: 10.1007/s12403-015-0170-x.

48 Y. Zhang, J. Wu and B. Xu, *Environ. Earth Sci.*, 2018, **77**(7), 273, DOI: 10.1007/s12665-018-7456-9.

49 D. Karunanidhi, P. Aravinthasamy, T. Subramani and K. Srinivasamoorthy, *Hum. Ecol. Risk Assess.*, 2019, **25**(1–2), DOI: 10.1080/10807039.2019.1568859.

50 T. Subramani, N. Rajmohan and L. Elango, *Environ. Monit. Assess.*, 2009, **162**(1–4), 123–137, DOI: 10.1007/s10661-009-0781-4.

51 World health statistics, *Monitoring health for the SDGs, Sustainable Development Goals*, World Health Organization, Geneva, 2017. Licence: CC BY-NC-SA 3.0 IGO.

52 T. Subramani, L. Elango and S. R. Damodarasamy, *Environ. Geol.*, 2005, **47**, 1099–1110.

53 C. P. Emenike, I. T. Tenebe and P. Jarvis, *Ecotoxicol. Environ. Saf.*, 2018, **156**, 391–402.

54 D. K. Todd, *Groundwater hydrology*, Wiley Publications, New York, 1980.

55 J. D. Hem, *U.S. Geological Survey Water Supply Paper 2254*, Scientific Publishers, Jodhpur, India, 1991, p. 264.

56 D. Karunanidhi, G. Vennila, M. Suresh and P. Karthikeyan, *Arabian J. Geosci.*, 2013, **7**(5), 1791–1798, DOI: 10.1007/s12517-013-0881-x.

57 K. Srinivasamoorthy, M. Chidambaram, M. V. Prasanna, M. Vasanthavigar, A. John Peter and P. J. Anandhan, *Journal of Earth System Science*, 2008, **117**(1), 49–58.

58 A. M. Piper, *Trans., Am. Geophys. Union*, 1944, **25**, 914–928.

59 D. K. Chadha, *Hydrogeol. J.*, 1999, **7**, 431–439.

60 A. L. Choi, G. Sun, Y. Zhang and P. Grandjean, *Environ. Health Perspect*, 2012, **1362**, 1362–1368.

61 T. Berger, F. A. Mathurin, H. Drake and M. E. Astrom, *Sci. Total Environ.*, 2016, 569–570, DOI: 10.1016/j.scitotenv.2016.06.002, 948–960.

62 J. Chen, H. Wu, H. Qian and Y. Gao, *Expo. Health*, 2017, **9**, 183–195.

63 R. J. Gibbs, Mechanisms controlling world water chemistry, *Science*, 1970, **170**, 795–840, DOI: 10.1126/science.170.3962.1088.

64 N. Adimalla and P. Li, *Hum. Ecol. Risk Assess.*, 2019, **25**(1–2), 81–103, DOI: 10.1080/10807039.2018.1480353.

65 O. A. Loni, F. K. Zaidi, M. S. Alhumimidi, O. A. Alharbi, M. T. Hussein, M. Dafalla, K. A. AlYousef and O. M. K. Kassem, *Arab. J. Geosci.*, 2014, DOI: 10.1007/s12517-014-1623-4.

66 D. Marghade, D. B. Malpe and A. B. Zade, *Environ. Monit. Assess.*, 2012, **184**, 2405–2418.

67 E. Fijani, A. A. Moghaddam, F. T.-C. Tsai and G. Tayfur, *Water Resources Management*, 2016, **31**(3), 765–780, DOI: 10.1007/s11269-016-1390-y.

68 H. Schoeller, *Geochemistry of groundwater. An international guide for research and practice*, UNESCO, 1967, ch. 15, pp. 1–18.

Paper

69 N. Toumi, B. H. Hussein and S. Rafrafi, *Environ. Monit. Assess.*, 2015, **187**(3), 1–16.

70 N. S. Rao, D. Marghade, A. Dinakar, I. Chandana, B. Sunitha, B. Ravindra and T. Balaji, *Environ. Earth Sci.*, 2017, **76**, 747.

71 P. J. Sajil Kumar, P. Jegathambal and E. J. James, *Environ. Earth Sci.*, 2014, **72**, 2437–2446.

72 N. Adimalla and H. Qian, *SN Appl. Sci.*, 2019, **1**, 202, DOI: 10.1007/s42452-019-0219-8.